Oct 20th, 12:00 AM

Calibration of a Bending Model for Cold-formed Sections

A. De Martino

A. Ghersi

Frederico M. Mazzolani

Eleventh International Specialty Conference on Cold-Formed Steel Structures
St. Louis, Missouri, U.S.A., October 20-21, 1992

CALIBRATION OF A BENDING MODEL FOR COLD-FORMED SECTIONS

De Martino A.[1] - Ghersi A.[1] - Landolfo R.[2] - Mazzolani F.M.[3]

ABSTRACT

The calibration procedure of a numerical model based on the simulation of the moment-curvature relation for cold-formed steel beams is presented. The results of bending tests on beams with double-channel cross-section are used to assess the proper values to the parameters which quantify the model.

1. INTRODUCTION

This paper is part of a general research project devoted to the study of the cold-formed thin-gauge sections, with the aim to provide useful data on the use of these profiles in seismic resistant structures [1, 2].

The first goal of this project was to define a consistent numerical model able to simulate the complete load-deformation (moment-curvature) history of this kind of sections, which are strongly affected by the local buckling of compressed parts. The proposed model considers the section subdivided in several small areas, which are characterized by a given stress-strain relationship and a residual deformation and are associated to all informations needed to follow step by step the evolution of the load versus deformation history. The arising of local buckling and the progressive modification of the buckled parts at the increase of the deformation is evaluated by means of different theoretical approaches which involve appropriate parameters such as those showing the effectiveness of the mutual restraint given by the contiguous elements (flanges, webs, lips) in the cross-section.

The analysis of the influence of such local buckling theoretical interpretations with their parameters and the calibration of the proposed model (i.e. the definition of the most suitable physical interpretation of local buckling and the evaluation of the numerical parameters involved) has already been carried out in the case of thin-gauge welded box-sections [3, 4, 5], for which some experimental results were available [6].

In case of double-channel thin-gauge beams the numerical analysis of their bending behaviour has been performed in the same way [7]. In the meantime bending tests on a series of simply supported double-channel cold-formed beams have been carried on at the "Laboratorio Prove Materiali Strutture" of the University of Ancona, Italy [8, 9]. These experimental results are shortly recalled here because they are used to calibrate the proposed model in the case of this kind of sections.

1 Associate Professor of Structural Engineering, University of Naples, Italy

2 Research Assistant, University of Naples, Italy

3 Professor of Structural Engineering, University of Naples, Italy

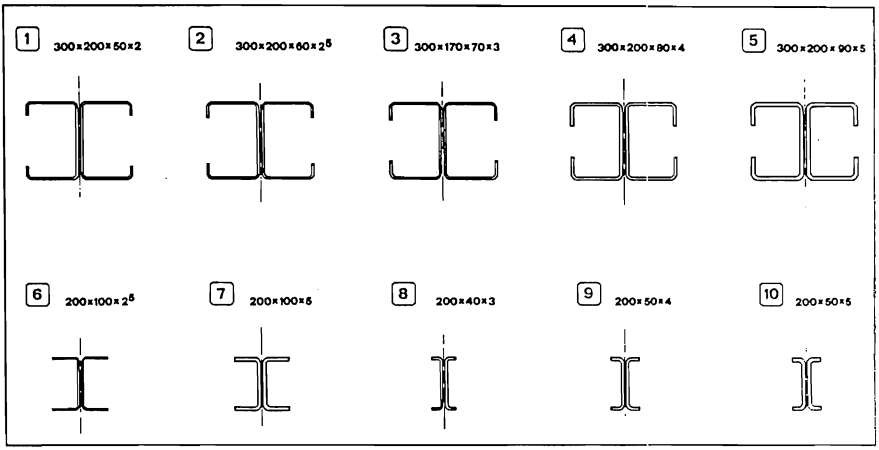
1 300×200×50×2
2 300×200×60×2.5
3 300×170×70×3
4 300×200×80×4
5 300×200×90×5
6 200×100×2.5
7 200×100×5
8 200×40×3
9 200×50×4
10 200×50×5

fig.1

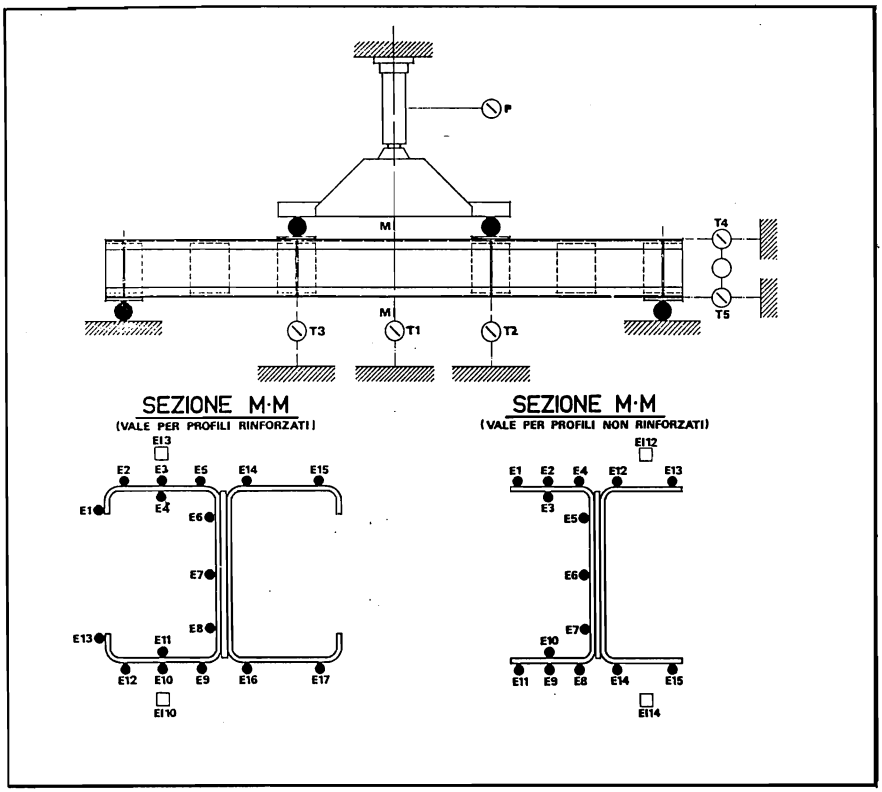
P
M
M
T1
T2
T3
T4
T5
SEZIONE M·M
(VALE PER PROFILI RINFORZATI)
E1 E2 E3 E4 E5 E6 E7 E8 E9 E10 E11 E12 E13 E14 E15 E16 E17
SEZIONE M·M
(VALE PER PROFILI NON RINFORZATI)
E1 E2 E3 E4 E5 E6 E7 E8 E9 E10 E11 E12 E13 E14 E15

fig.2

2. EXPERIMENTAL RESULTS

The experimental investigation has been carried out on 10 specimens made of Fe360 steel ($f_y = 235$ N mm^{-2}), composed by two back to back coupled cold-formed channels, with or without stiffening lips, named P1 to P10 (fig.1). Cross-sections were designed to cover a wide range of *w/t* ratio values, going from plastic (P10), compact (P5), semi-compact (P8, P9) to slender (P1, P2, P3, P4, P6, P7) sections, according to the classification of Eurocode n.3 [10].

Monotonic tests were performed on simply supported beams, 3.00 m of span, by imposing displacements and measuring the corresponding forces, applied in two points, 1.00 m distant across the mid-span (fig.2). They were finalized to obtain informations both on the overall behaviour parameters of the member (ultimate moment, rotational capacity, vertical displacement) and on the local behaviour parameters of the mid-span cross-section (development of stress and strain, measured also in the post-critical field, until the overall collapse). The lack of planarity of the cross section in the last stage of tests made necessary to discard the values of the most disturbed gauges, evaluating for each specimen a set of moment-curvature curves, numerically obtained by considering different groups of strain gauges for the definition of the curvature values (fig.3).

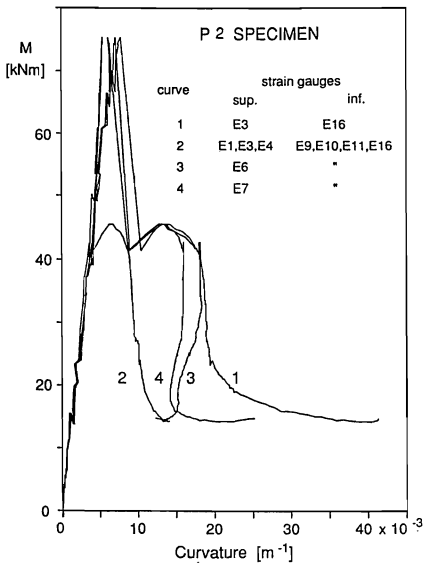

fig.3

The load-deflection and moment-curvature curves put in a great evidence the different behaviour of stiffened versus unstiffened sections (fig.4). The presence of edge stiffeners (P1-P5 specimens) increases the load carrying capacity of the beam and allowes a nearly linear behaviour up to the maximum load (fig.4a); however, their buckling reduces the restraint of the compressed flanges, causing an immediate loss of load carrying capacity. On the contrary, flange buckling in unstiffened sections (P6-P10 specimens) appeares to be more progressive, with a slower reduction of strength in the softening branch of the curve (fig.4b). As a consequence, the choice of a design moment M_d significantly lower than the observed one M_{exp} may give very different ductility levels, depending on the presence or absence of stiffening lips.

Further differences were pointed out by the analysis of experimental results, related to the interaction between local and global buckling.

In fact some unstiffened specimens (P8-P10) showed a torsional-flexural buckling which immediately followed the local buckling of the flanges [11].

For all these reasons, the calibration procedure has been carried out separately for stiffened and unstiffened sections. The first ones needed a more detailed analysis of the buckling interaction among the different elements of the section, which required an improvement of the proposed model. The second ones needed the evaluation of the torsional-flexural buckling, which confirmed the experimental evidence, but could not be included in the model, which is related only to the behaviour of the section.

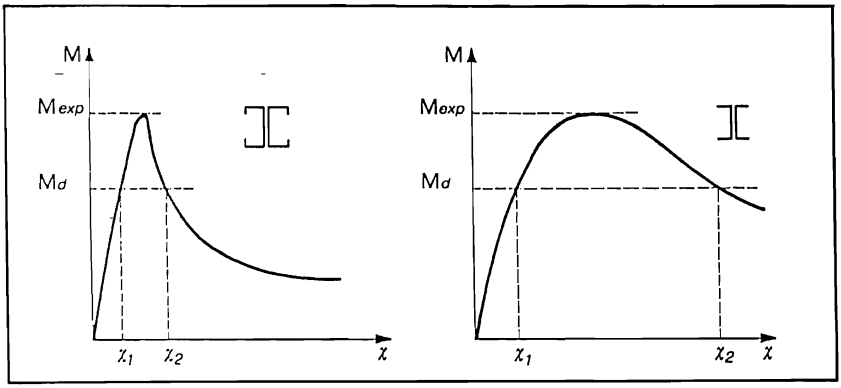

fig.4, a *fig.4, b*

3. STIFFENED SECTIONS

The main problem in the theoretical or numerical analysis of stiffened sections is the evaluation of the actual capability of the edge stiffener to restrain the compressed flange and thus to postpone its local buckling. Depending on the lip size, the behaviour of the section ranges within two limit conditions: fully effective restraint, which allows the flange to behave as connected to two webs; uneffective restraint, which makes the flange to behave as having a free edge.

The Italian code for cold-formed steel sections [12], following the 1980 AISI Specification [13], prescribes a minimum length D of the stiffener related to the thickness t and to the width w of the flange by means of the condition

$$D \geq \beta t$$

where

$$\beta = 2.8\sqrt[6]{\left(\frac{w}{t}\right)^2 - \frac{27400}{f_y}}$$

and f_y is the yield stress, expressed in N mm^{-2}. When this condition is fulfilled the stiffener is considered fully effective, even when its slenderness ratio D/t is such as to permit its local buckling and then to require the evaluation of its statical contribute by means of a reduced effective area.

The 1986 AISI Specification [14] defines an optimum width and an adequate moment of inertia I_a of the stiffener, related to the dimensions w and t of the flange. Both a smaller size of the stiffener ($I_s < I_a$) and a bigger one ($D/w > 0.25$) reduce the restraint effectiveness; formulations are therefore provided to evaluate in these cases a value of the plate buckling coefficient k smaller than the one corresponding to a fully effective stiffener.

Nevertheless, some recent tests [15] showed that in the case of wide stiffening lips the AISI formulations are unsafe, pointing out the necessity of assessing an upper limit to the stiffener width D. In the above mentioned paper, the following limits were proposed:

$$D/t < 14 \qquad \text{and} \qquad D/w < 0.4$$

In the tested specimens the stiffener size, ranging from 50 to 90 mm, always exceeds the D/t limit; also the D/w limit is slightly overcome in sections P3 and P5. For this reason, the first problem to be examined in the calibration of the model is concerned to the entity of the restraint given by the stiffener to the compressed flange. The numerical model proposed in [3] analyses the local buckling of each compressed element by means of many theoretical approaches, all of them requiring the definition of the plate buckling coefficient k. The assumption of a value k=4 for the compressed flange and k=7.81 for the web (i.e. the values for a plate simply supported at the edges with constant and linear load respectively) gives a maximum moment significantly greater than the experimental one (fig.5, curve *a*, related to the P2 specimen). On the other side a value k=0.43 for the flange (i.e. the value for an element having one edge simply supported and the other one free) shows an early arising of the local buckling, with a subsequent non-linear behaviour, and a maximum moment lower than the measured one (fig.5, curve *b*). In both cases the moment-curvature diagrams have a decreasing branch similar to the experimental one, but not enough steep.

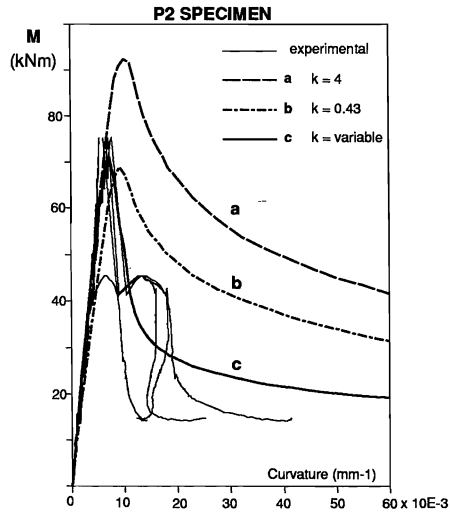

fig.5

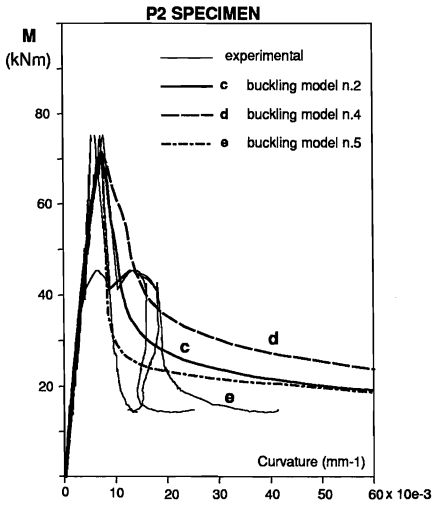

fig.6

The comparison between numerical and experimental values suggests that:

- the linear behaviour of the compressed flange in the first stage of loading is well described by the scheme of plate supported at both edges (k=4);
- the difference in the maximum moment is connected to the progressive buckling of the stiffener and may be simulated by a gradual reduction of the buckling coefficient of flange;
- the steepness of the experimental decreasing branch can not be numerically obtained only by means of reduced values of the flange buckling coefficient; it is then necessary to assume a progressive reduction for the k coefficient of the web, connected to the contemporary buckling of the flange.

These considerations bring to the opportunity to modify the numerical model with the introduction of a variable buckling coefficient. The restraint effectiveness coefficient r has therefore been defined as the ratio of the effective width b to the geometrical width w of the element which gives the restraint (the lip for the flange and the flange itself for the web):

$$r = \frac{b}{w}$$

The limit value r=1 indicates a fully effective restraint, to which corresponds a value of the buckling coefficient k=k_1, while r=0 denotes the absence of restraint and thus a lower value of k (k=k_0). A quadratic relation between r and k has been assumed in order to express the reduction of the critical load corresponding to a decreased effectiveness of the restraint:

$$k = (k_1 - k_0)\, r^2 + k_0$$

The numerical results obtained in this way are enough satisfying, but for a better consistency of the model also the reciprocal influence of web to flange and flange to lip has been considered. The flange buckling coefficient has therefore assumed to depend on the restraint effectiveness coefficient of lip r_l and of web r_w. The limit values r_l=1 and r_w=1 indicate a fully effective restraint at both edges, to which corresponds a value of the buckling coefficient k=$k_{1,1}$; the values r_l=0 and r_w=1 denote the absence of restraint at the edge connected to the lip and give the value k=$k_{0,1}$ which has been assumed equal to the value $k_{1,0}$ corresponding to the absence of restraint at the edge connected to the web; finally, the values r_l=0 and r_w=0 indicate the uneffectiveness of both restraints, to which corresponds a value of the buckling coefficient k=$k_{0,0}$. An exponential relation between r_l, r_w and k has been assumed

$$k = a\left(\frac{r_l + r_w}{2}\right)^n + c$$

The parameters a, c and n have been evaluated by imposing the limit conditions

$$k = k_{1,1} \quad \text{when} \quad r_l = 1 \quad \text{and} \quad r_w = 1$$

$$k = k_{0,1} = k_{0,1} \quad \text{when} \quad r_l = 0 \quad \text{and} \quad r_w = 1$$

$$\text{or} \quad r_l = 1 \quad \text{and} \quad r_w = 0$$

$$k = k_{0,0} \quad \text{when} \quad r_l = 0 \quad \text{and} \quad r_w = 0$$

obtaining

$$a = k_{1,1} - k_{0,0}$$

$$c = k_{0,0}$$

$$n = \log_2\left(\frac{k_{1,1} - k_{0,0}}{k_{0,1} - k_{0,0}}\right)$$

The numerical results obtained assuming k_1=7.81 and k_0=0.57 for the web, $k_{1,1}$=4, $k_{0,1}$=0.43 and $k_{0,0}$=0.43/2 for the flange, k_1=0.43 and k_0=0.43/2 for the lip show the best agreement with the experimental ones, both for the maximum moment and for the decreasing branch slope (fig.5, curve *c*). The use of upper limit values of the flange buckling coefficient slightly different from 4, corresponding to an intermediate situation between the simply supported and the fixed end, as suggested in [4, 5, 16], gives moment-curvature diagrams nearly coincident with curve *c*, appearing thus to be unimportant.

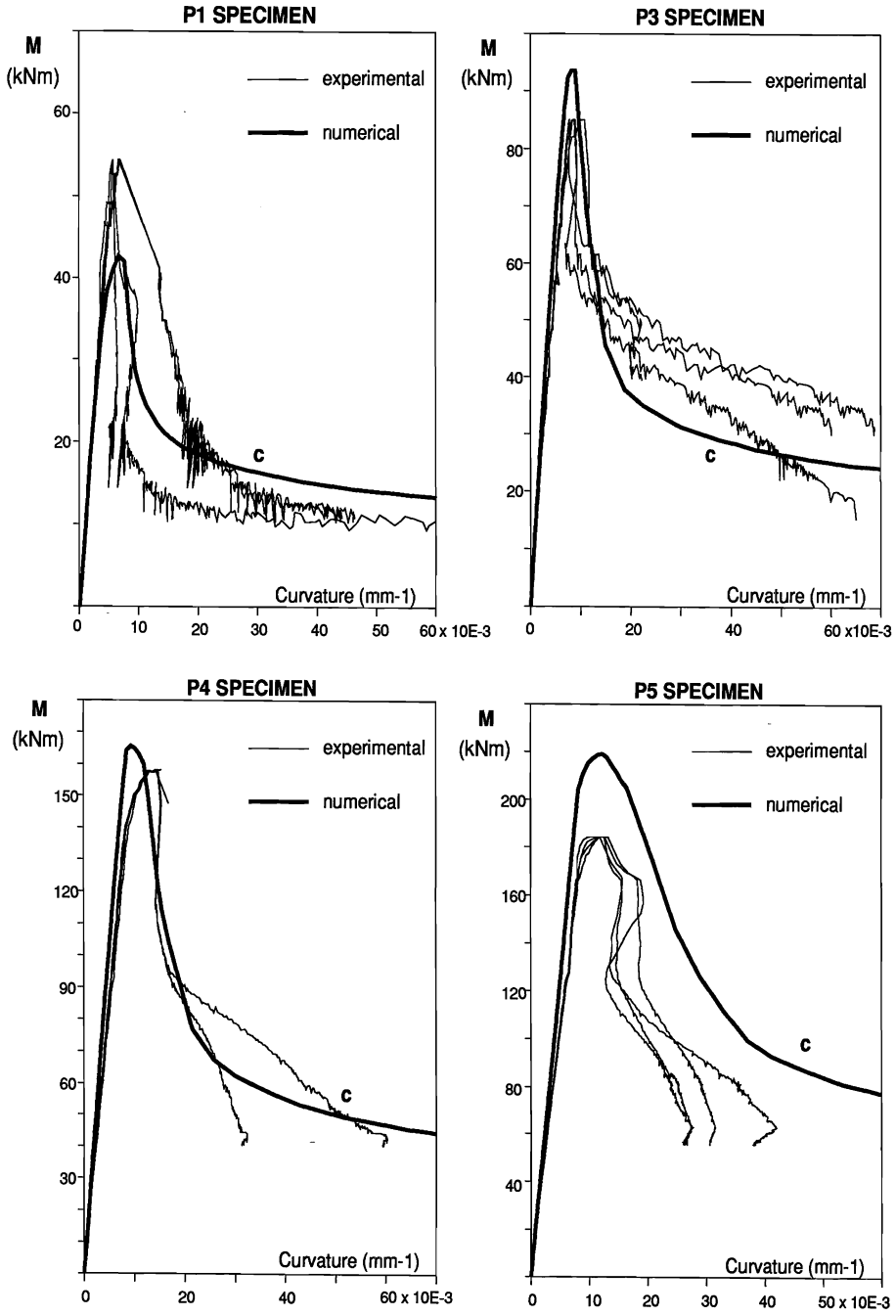
P1 SPECIMEN
M
(kNm)
experimental
numerical
60
40
20
c
Curvature (mm-1)
0
10
20
30
40
50
60 x 10E-3
P3 SPECIMEN
M
(kNm)
experimental
numerical
80
60
40
20
c
Curvature (mm-1)
0
20
40
60 x10E-3
P4 SPECIMEN
M
(kNm)
experimental
numerical
150
120
90
60
30
c
Curvature (mm-1)
0
20
40
60 x 10E-3
P5 SPECIMEN
M
(kNm)
experimental
numerical
200
160
120
80
40
c
Curvature (mm-1)
0
10
20
30
40
50 x 10E-3

fig.7

The calibration step immediately following the assessment of the plate buckling coefficient has been the comparitive analysis of the results given by the different theoretical approaches of local buckling allowed by the numerical model. The up to now shown curves are obtained by means of the relations provided by the buckling model n.2 in [3, 5], which extends to the post-yielding field the elastic formulation of critical load in term of strain. The approaches indicated in the same papers as n.4 (relations derived by the authors on the base of formulations given by Kemp, Lay and Galambos) and as n.5 (expressions obtained on the base of some experimental data) produce moment-curvature curves with slightly different slope of the falling branch (fig.6, curves *d* and *e* respectively); although the use of curve *e* may be suggested as the most safe, curve *c* appears to be still the most consistent with the experimental data.

A further theoretical problem examined in [3, 5] was the progressive modification of the buckled part, which may be analysed considering each compressed element as composed of a set of fibres for which the slenderness is related to the distance from the edge. The numerical analyses performed show that for this kind of cross-sections the linear variation of this parameter (assumed in the evaluation of the diagrams in fig.5 and 6) is preferable to the non linear relations, which give moment values significantly higher than the experimental ones because of the slower progression of local buckling.

All numerical analyses were carried on by assuming the usual elastic perfectly plastic stress-strain relationship, without hardening; the influence of geometrical imperfections on local buckling was taken into account by decreasing the effective width of the compressed elements by means of the well known expression proposed by Winter.

In figure 7 are shown the numerical results obtained in the same way for the P1, P3, P4 and P5 specimens. The curves corresponding to P3 and P4 beams appear to be in a remarkable agreement with the experimental data both for the maximum moment value and for the steepness of the decreasing branch. A lesser accordance may be noted in the case of P1 and P5 specimens. In fact, in both cases the shape of the diagram is quite adequate but the simulated values of the maximum moment differ from the experimental ones in opposite way. In case of P1 specimen, which is the most slender section, the numerical model provides a maximum moment about 20% less than the experimental one; a better concordance could be achieved only postponing local buckling, i.e. using an higher value of the plate buckling coefficients. On the contrary, in case of P5 specimen, which has a compact section, the numerical model over-estimates the maximum moment, showing that probably the restraint provided by the stiffening lip is less effective than what expected and that the model should then require a lower buckling coefficient.

4. UNSTIFFENED SECTIONS

As explicitly declared in [8], the experimental behaviour of some unstiffened specimens was affected by their flexural-torsional buckling. In fact the arising of local buckling in the compressed flange of P8, P9 and P10 beams gave rise to a lateral displacement which gradually increased together as far as the increase of the imposed vertical displacement.

Taking into account the flexural-torsional buckling, the elastic critical moment M_e evaluated according to 1986 AISI Specification is smaller than the yielding moment M_y in case of P8 specimen and only slightly greater in case of P9 and P10 specimens. The critical moment M_c is therefore significantly different from the yielding moment, while the effect of local buckling in the evaluation of the nominal moment M_n is less important, because of the compactness of their cross-sections.

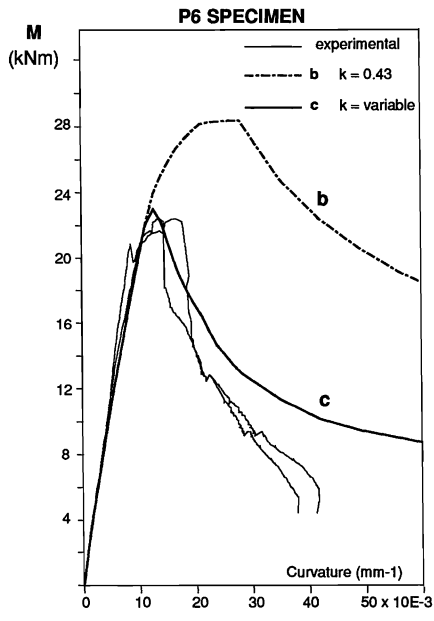

fig.8

The flexural-torsional buckling might have slightly affected also the behaviour of P7 specimen, even if no relevant horizontal displacement was noted during the test. In fact the nominal moment evaluated considering lateral buckling is slightly smaller than the value corresponding only to local buckling.
The effect of flexural-torsional buckling cannot be directly introduced in the proposed model, which is referred to the behaviour of the section not of the beam as a whole. For this reason, the comparison between experimental and numerical values has been pursued only with regard to P6 specimen. In fact only in this case of unstiffened profile the high slenderness of the flange (b/t=40) produced a premature local buckling before reaching the overall one. Figure 8 shows the curve *b*, corresponding to constant values of the buckling coefficients (k=0.43 for the unstiffened flange, k=7.81 for the web), and the curve *c*, for which the buckling coefficients vary in the way shown in the previous section.
The progressivereduction of k gives also in this case a good accordance both for the maximum moment and for the decreasing branch.

5. CONCLUSIONS

The present analysis has emphasized the role played by the different theoretical approaches to local buckling and by the numerical parameters involved, in the case of cold-formed beams with double channel cross-section. The improvement of the model proposed in previous papers allowed a good agreement of numerical results versus experimental data. After calibration, the model is ready to allow a parametric analysis of this kind of sections, in order to obtain more detailed informations on its bending behaviour.

APPENDIX - REFERENCES

1. De Martino A., De Martino F.P., Ghersi A., Mazzolani F.M., Il comportamento flessionale di profili sottili sagomati a freddo: impostazione della ricerca, Acciaio, September 1989, pp.415-422.
2. De Martino A., De Martino F.P., Ghersi A., Mazzolani F.M., Il comportamento flessionale di profili sottili sagomati a freddo: ricerca teorico-sperimentale, XII Congresso C.T.A., Capri, October 1989, pp.535-547.
3. De Martino A., Ghersi A., Mazzolani F.M., Analisi dei parametri di influenza del comportamento flessionale delle sezioni a cassone in parete sottile, XII Congresso C.T.A., Capri, October 1989, pp.521-354.

4. De Martino A., Ghersi A., Mazzolani F.M., Calibration of a bending model for thin walled steel box-section, International Colloquium on Stability of Steel Structures, Budapest, April 1990.
5. De Martino A., Ghersi A., Mazzolani F.M., On the bending behaviour of thin walled box-sections, Costruzioni Metalliche, n.6, 1991, pp.347-360.
6. Ballio G., Calado L., Sezioni inflesse in acciaio sottoposte a carichi ciclici. Sperimentazione e simulazione numerica, Costruzioni Metalliche, n.1, 1986.
7. De Martino A., Ghersi A., Mazzolani F.M., Bending behaviour of double-C thin walled beams, X International Specialty Conference on Cold-Formed Steel Structures, St.Louis, Missouri, October 1990, pp.637-648.
8. De Martino A., De Martino F.P., Ghersi A., Mazzolani F.M., Il comportamento flessionale di profili sottili sagomati a freddo: indagine sperimentale, Acciaio, December 1990, pp.577-588.
9. De Martino A., De Martino F.P., Ghersi A., Mazzolani F.M., Bending behaviour of double-C thin-gauge beams: experimental evidence versus codification, 4th International Colloquium on Structural Stability, Mediterranean Section, Istanbul, September 1991.
10. Eurocode n.3, Design of Steel Structures, 1990.
11. Ghersi A., Landolfo R., Mazzolani F.M., Buckling modes of double C cold-formed beams, First International Specialty Conference on Coupled Instabilities in Metal Structures, Timisoara, October 1992.
12. CNR 10022, Profili formati a freddo: Istruzioni per l'impiego nelle costruzioni, 1984.
13. American Iron and Steel Institute, Specification for the Design of Cold-Formed Steel Structural Members, Cold-Formed Steel Design Manual, 1980.
14. American Iron and Steel Institute, Specification for the Design of Cold-Formed Steel Structural Members, Cold-Formed Steel Design Manual, August 1986 with December 1989 Addendum.
15. Willis C.T., Wallace B.J., Wide lips - a problem with the 1986 code, X International Specialty Conference on Cold-Formed Steel Structures, St.Louis, Missouri, October 1990, pp.441-450.
16. Landolfo R., Sul comportamento flessionale dei profili sottili formati a freddo, P.h.D. Dissertation, Naples, 1992.

APPENDIX - NOTATION

b effective width of compressed flange
D stiffener width
f_y yield stress of steel
k buckling coefficient
k_0 buckling coefficient for an element with one edge free
k_1 buckling coefficient for an element with both edges restrained
I_a adequate moment of inertia of stiffener
I_s actual moment of inertia of stiffener
r restraint effectiveness coefficient
r_l lip restraint effectiveness coefficient
r_w web restraint effectiveness coefficient
t element thickness
w flange or web thickness